

### PHASE STABILITY STUDY OF CrFeCoNiCu HIGH ENTROPY ALLOY

---

This chapter deals with the synthesis, characterization and thermal stability of the equiatomic CrFeCoNiCu high entropy alloy. Among the HEAs, CrFeCoNiCu system has been reported earlier [24,32,91,105–107]. Al and Ti are generally added to this alloy in varying amounts to study the phase evolution and mechanical properties. Most of the studies on these alloy systems are carried out on as-cast samples [91]. Praveen *et al.* [24] and Thangaraju *et al.* [91] have studied this system by mechanical alloying route followed by sintering. They have reported the presence of the  $\sigma$  phase after sintering the alloy. However, Thangaraju *et al.* [91] have not reported any  $\sigma$  phase formation after sintering. Due to these conflicting results on phase stability, it is important to reassess the thermal stability and evolution of the  $\sigma$  phase in CrFeCoNiCu system. In the present context, the phase stability of this HEA is studied by experimental and theoretical methods.

#### 3.1. Parametric approaches for the phase stability study

In the parametric approach, the important parameters such as enthalpy of mixing ( $\Delta H_{mix}$ ), the entropy of mixing ( $\Delta S_{mix}$ ), atomic radius difference ( $\delta$ ) and valence electron concentration (VEC) are calculated for the selected alloy system to find out whether it will form a single phase or mixture of phases. The literature on the phase stability of HEAs suggests that these parameters play a significant role in predicting a single phase disordered solid solution. For quinary and higher order systems, a single phase solid solution can be expected for  $-11.6 \text{ kJ.mol}^{-1} < \Delta H_{mix} < 5 \text{ kJ.mol}^{-1}$ , while  $\Delta S_{conf} \geq 1.61 \text{ R}$  [8,38,108]. The binary interaction parameters,  $\Omega_{ij}$ , obtained from the calculated mixing enthalpy using Miedema's model are used to estimate the integral molar enthalpy of

mixing for multi-component alloy solutions [21],  $\Delta H_{mix}$ , which is similar to a regular solution model.

The mixing enthalpy of a multi-component alloy consisting of N elements can be calculated using **Equation 1.11**. The calculated values for mixing enthalpy of the binary subsystems are given in **Table 3.2**, while the parameters used in the calculations of enthalpy of mixing for solid solution are given in **Table 3.1**. The  $\Delta H_{mix}$  value calculated for the quinary HEA ( $2.35 \text{ kJ.mol}^{-1}$ ) is well within the specified range for forming solid solution phase ( $-11.6 \text{ kJ.mol}^{-1} < \Delta H_{mix} < 3.2 \text{ kJ.mol}^{-1}$ ) [109]. From **Table 3.2**, it can be seen that all the binary systems (other than those containing Cu) except Co-Ni have small negative values of enthalpy of mixing, favors formation of solid solution phase. The ideal configurational entropy of the quinary alloy can be estimated by **Equation 1.14**.

As all the elements are from the 3d transition series, the atomic size difference calculated using **Equation 1.15** for solid solution formation is equal to 1.03, which is much smaller than 6.6, indicating the possibility of the formation of a solid solution.

Valance electron concentration (VEC) also plays a critical role in determining whether the disordered BCC, FCC, or mixture of two phases forms. For an N component system, the VEC is estimated by **Equation 1.16**.

It has been shown that a single phase FCC solid solution forms for  $VEC \geq 8$ , whereas a single phase BCC solid solution is expected for  $VEC \leq 6.8$  [37,68]. For intermediate values of VEC, a two-phase mixture of FCC and BCC phases is expected. VEC represents the total number of electrons in the valence band, including the d-electrons. The calculated values of the parameters, as mentioned above, are given in **Table 3.3**. Many researchers [3,21,108,110] have pointed out that enthalpy and the atomic size difference play a dominant role in the formation of a solid solution in HEAs compared to the entropy effect. For the system chosen, both these parameters are found to be within a

solid solution forming range. In the present context, the VEC value (8.80) is indicating the possible formation of the FCC phase.

**Table 3.1:** Parameters used in Miedema’s model for calculation of mixing enthalpy.

Element	$n_{ws}$	$n_{ws}^{1/3}$	$\phi$	V	$V^{2/3}$
Co	5.36	1.75	5.1	6.7	3.55
Cr	5.18	1.73	4.65	7.23	3.74
Cu	3.18	1.47	4.45	7.12	3.70
Fe	5.55	1.77	4.93	7.09	3.69
Ni	5.36	1.75	5.2	6.6	3.52

**Table 3.2:** The chemical mixing enthalpies  $\Delta H_{mix}^{ij}$  (kJ.mol<sup>-1</sup>) calculated using Miedema’s model for the present binary subsystems in equiatomic CrFeCoNiCu high entropy alloy.

Elements	Cu	Co	Cr	Fe	Ni
Cu	-	5	11	11	3
Co	5	-	- 4	-1	0
Cr	11	- 4	-	-1	-6
Fe	11	-1	-1	-	-1
Ni	3	0	-6	-1	-

**Table 3.3:** Calculated values of the parameters playing an essential role in phase stability.

Alloy	$\Delta H_{mix}$ (kJ.mol <sup>-1</sup> )	$\Delta S_{mix}$ (J.mol <sup>-1</sup> )	$\delta$ (%)	VEC	$\Delta\chi$
CrFeCoNiCu	2.35	13.40	1.03	8.80	0.09

3.2 Phase prediction based on DFT calculations

We have generated an eight atom special quasi-random structure (SQS) for the chosen alloy to mimic the random distribution of atoms in binary systems, as discussed in Chapter 2. The enthalpies of formation for the equiatomic binary alloys are shown in Table 3.4. The enthalpy values for all the three prominent crystal structures are calculated and tabulated.

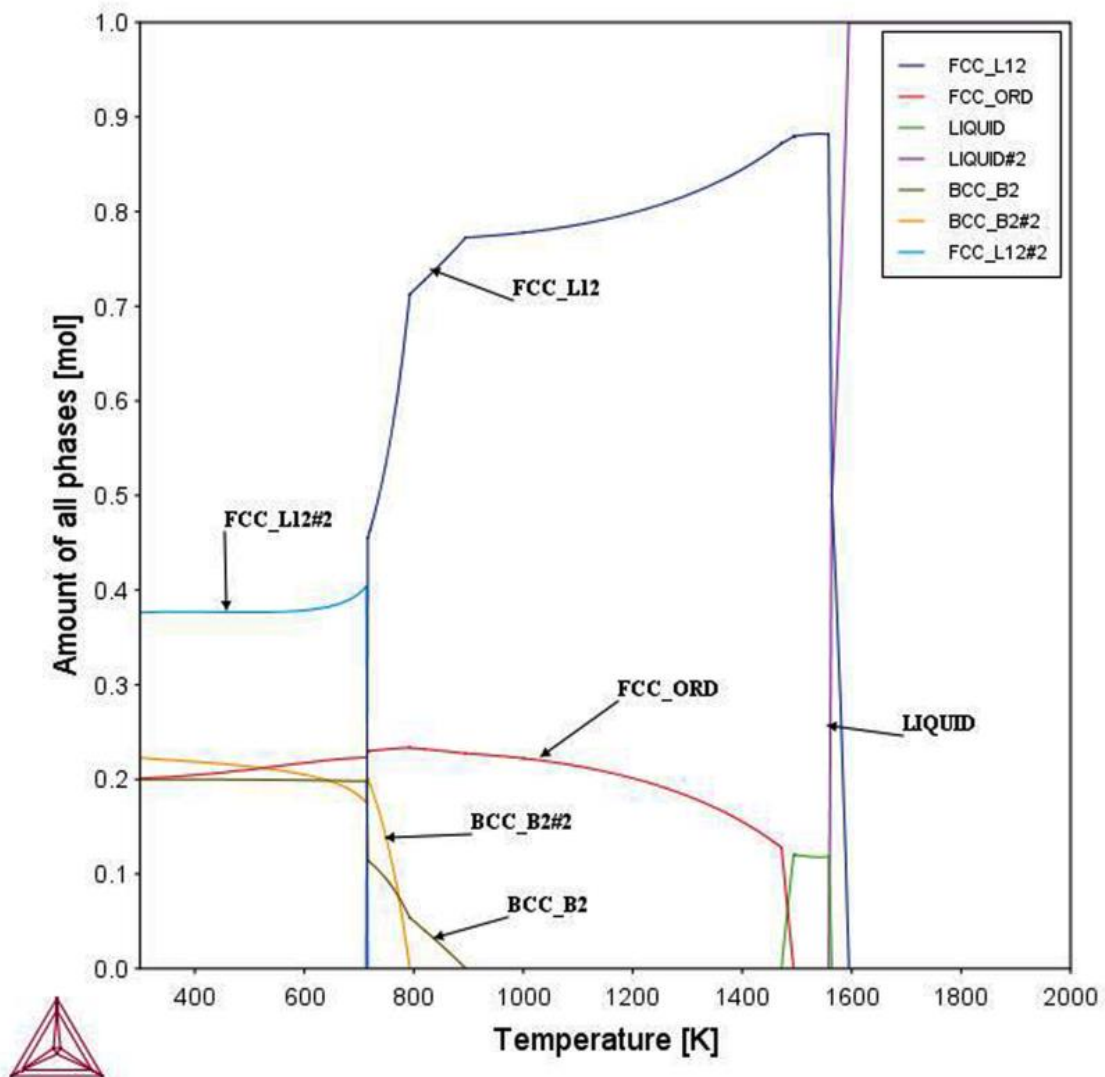


Figure 3.1: Prediction of amount of phases that may form with increasing temperature.

### Chapter 3 Phase Stability Study of CrFeCoNiCu High Entropy Alloy

A regular solution model is used to extrapolate the enthalpies of binary systems to predict the enthalpy of formation for the quinary alloy. From this table, one can easily recognize that the FCC phase is the stable phase. However, the enthalpy of the formation being positive certainly indicates phase separating tendency in the FCC phase. Thus there is a greater probability for the formation of multiple phases. However, the likelihood of formation of the FCC phase among other phases is quite prominent. The prediction of DFT does not conform the prediction done by the parametric approach, which indicates a single-phase FCC solid solution, whereas DFT predicts more than one solid solution phase.

**Table 3.4:** Enthalpy values for all binary subsystems in CrFeCoNiCu HEA calculated using DFT.

Binary subsystems	BCC ( $\Delta H_{mix}^{ij}$ , kJ.mol <sup>-1</sup> )	FCC ( $\Delta H_{mix}^{ij}$ , kJ.mol <sup>-1</sup> )	HCP ( $\Delta H_{mix}^{ij}$ , kJ.mol <sup>-1</sup> )
Co-Cr	2.865	3.350	-9.481
Co-Cu	18.14	16.557	14.007
Co-Fe	17.478	-5.683	-0.591
Co-Ni	0.180	0.022	2.461
Cr-Cu	29.496	28.926	34.175
Cr-Fe	8.103	11.610	15.997
Cr-Ni	4.963	4.040	4.045
Cu-Fe	16.141	13.850	14.386
Cu-Ni	5.656	4.206	2.181
Fe-Ni	-7.032	-7.032	-0.237
$\Delta H_{mix}^{DFT}$ (kJ mol <sup>-1</sup> )	15.358	11.175	16.711

**3.3 Phase prediction based on CALPHAD**

The thermo-Calc software has been used to predict the number of phases that may form with increasing temperature (**Figure 3.1**). We can observe that two ordered phases are stable at a high temperature below solidus temperature from the figure. It can be shown that the B2 phase starts precipitating from the FCC\_L12 phase at ~900 °C. At around 800 °C, another B2 phase is precipitating from the FCC\_L12 phase, as indicated in **Figure 3.1**. Single point calculation shows the composition of phases at 500 °C and 1000 °C, shown in **Table 3.5**. From the table, it is clear that BCC\_B2#1 is Cr rich phase with small amount of Fe. However, BCC\_B2#2 Fe and Co rich phase with small amount of Cr and Ni in it. Two ordered FCC phase formed are FCC\_L12 and FCC\_ORD. The FCC\_L12 structure is Ni rich phase with reasonable amount of Fe and Co at 500 °C temperature, whereas approximately equal composition of Cr, Fe Co and Ni at 1000 °C. The FCC\_ORD is a immiscible Cu rich phase with small amount of Co in the matrix.

**Table 3.5:** Composition of phases at 500 °C and 1000 °C, calculated using single point calculation tool of Thermo-Calc (SSOL\_5 database).

Temp. (°C)	Phase	Phase Frac.	Cr	Fe	Co	Ni	Cu
<b>500</b>	BCC_B2#1	0.199	0.998	0.002	0	0	0
	BCC_B2#2	0.214	0.003	0.488	0.504	0.003	0
	FCC_L12#2	0.376	0	0.253	0.213	0.529	0.003
	FCC_ORD	0.210	0	0	0.056	0	0.944
<b>1000</b>	FCC_L12#1	0.778	0.257	0.257	0.213	0.257	0.015
	FCC_ORD	0.222	0	0	0.153	0	0.847

**3.4 Experimental results on phase evolution in the milled powder**

The quinary CrFeCoNiCu HEA was mechanically milled for up to 65 h. The evolution of the phases at regular intervals of milling time has been studied through XRD.

The diffraction patterns corresponding to the different milling times are displayed in **Figure 3.2**. At the initial blending of powder (i.e., milling for 10 min.), diffraction peaks corresponding to every constituent element could be identified, showing the presence of all the alloying elements in the starting mixed powder material. The diffraction intensities of all the constituent elements decrease with the broadening of the peaks with increasing milling time. The peaks intensity corresponding to (100) and (101) planes of Co and (200) plane of Ni reduced significantly after 10 h of milling, which disappeared entirely after 30 h of milling. It can be seen that most of the peaks lose their identity except those corresponding to Fe/Cr and Cu. As the lattice parameters of the Fe and Cr are very close, corresponding peaks overlap. This suggests that a solid solution has formed by the dissolution of Co and Ni in Fe/Cr lattice. It appears that Co and Ni dissolves in Fe or Cr host lattice to form the BCC phase having lattice parameters close to Fe/Cr. Due to a reduction in the crystallite size and increasing internal strain, there is a significant reduction in all the higher-order peak intensities. No further changes occur in the diffraction pattern of the powder milled for 50-65 h other than the formation of a two-phase structure.

Crystallite size and strain have been determined using Scherrer's method [111], in which the following equations estimate the peak broadening  $B$  due to crystallite size and internal strain.

$$B_{crystallite} = \frac{k\lambda}{L \cos\theta} \quad (3.1)$$

$$B_{strain} = \eta \tan\theta \quad (3.2)$$

where  $L$  is the average crystallite size,  $\eta$  strain-induced due to MA,  $k$  a constant (which in general is equal to 1.0), the Pseudo-Voigt method was followed for peak fitting, and then

the FWHM of the prominent peak was measured [112]. The decrease in crystallite size with increasing lattice strain concerning milling time is displayed in **Figure 3.3**.

The milled powder morphology for 65 h has been studied through scanning electron microscopy (SEM), as shown in **Figure 3.4**. It could be observed that the particles are mostly flaky in nature, and their sizes vary in the range of 2 to ~ 10  $\mu\text{m}$  with a few exceptions of 15 to ~20  $\mu\text{m}$ , as shown in **Figure 3.6**. This flaky nature of the particles is due to the heavy deformation involved during the mechanical working of the powder. The SEM-EDX analysis of the 65 h milled powder is found to be close to the nominal composition of the alloy, as discussed in **Figure 3.6**. It suggests that the milled powder is homogeneous in composition.

The existence of two phases can also be confirmed on indexing the selected area diffraction (SAD) patterns obtained through transmission electron microscopy. The bright field (BF) and corresponding selected area diffraction (SAD) pattern of the 65 h milled powder is shown in **Figure 3.7** (a) and (b). Indexing of the SAD pattern confirms the BCC solid solution phase ( $a = 2.85 \pm 0.02 \text{ \AA}$ ). A diffuse ring of minor FCC ( $a = 3.60 \pm 0.02 \text{ \AA}$ ) crystal. **Figure 3.7** (c) showed the dark field image of the same area. It could be ascertained that a large fraction of the particles has sizes in the nanometer range. This is consistent with the fact that MA is well known for producing nanostructured materials. Formation of the uniform rings in SAD pattern indicates that the alloy particles are nanosized and randomly oriented in the alloy matrix. These results further corroborate the phase evolution by XRD analysis of the 65 h milled powder.

The STEM-EDS elemental mapping of 65 h milled powder is displayed in **Figure 3.8**. It has been found from the elemental mappings that Fe, Cr, Co, Cu, and Ni are alloyed to form the BCC phase while some Cu remains unalloyed in the matrix as a minor FCC phase.



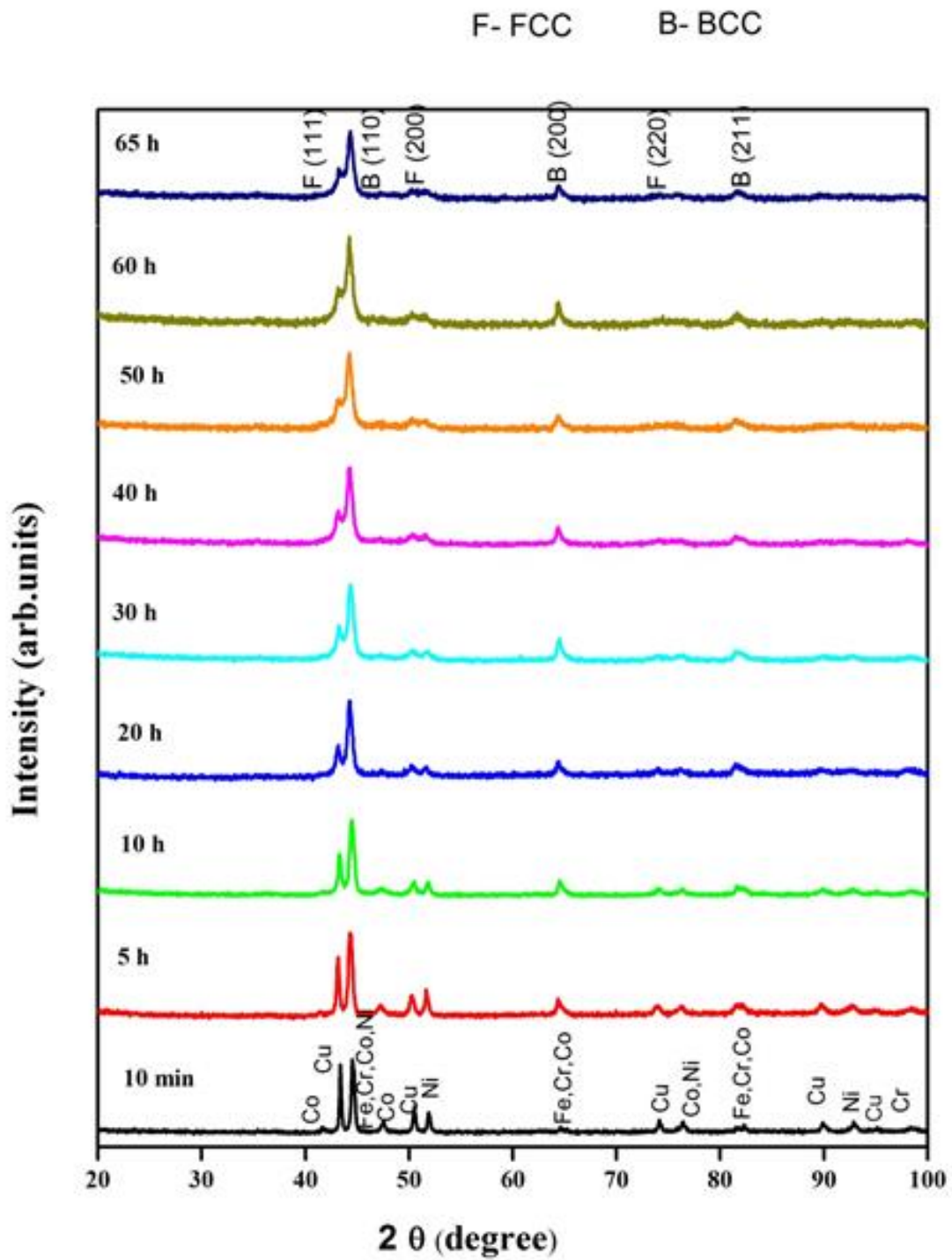


**Figure 3.2:** XRD patterns of CrFeCoNiCu HEA powders as a function of milling time. After milling for 10 min., diffraction peaks corresponding to every constituent element could be identified. The final peaks (65 h) show the major BCC and minor FCC phase.

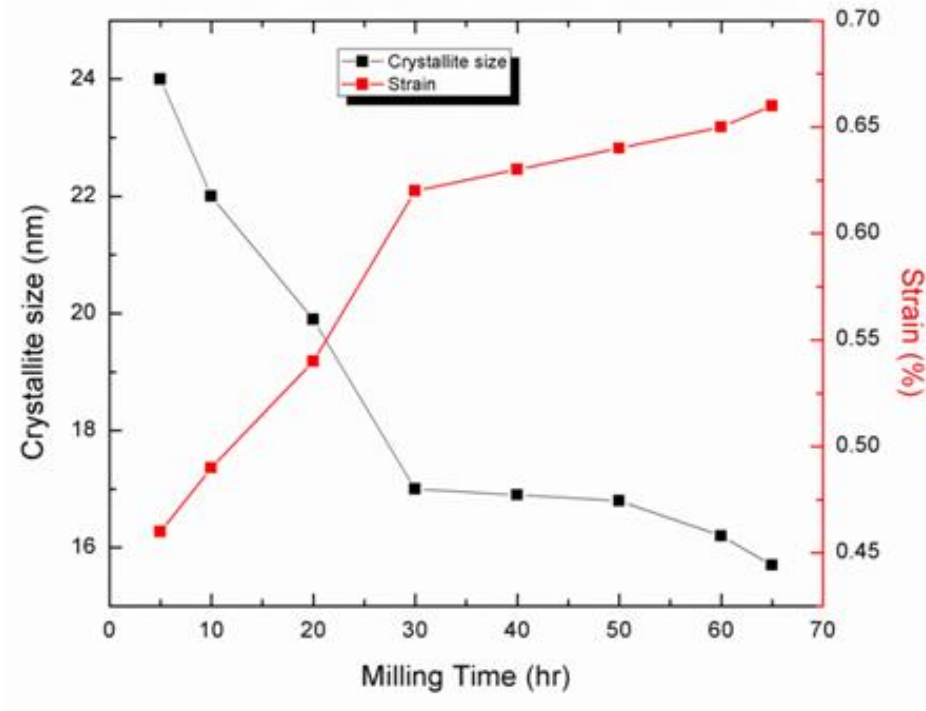


**Figure 3.3:** Variation of crystallite size and lattice strain has been shown as a function of milling time for BCC phase. It shows that crystallite size decreases with increases in lattice strain as milling proceeds with time.

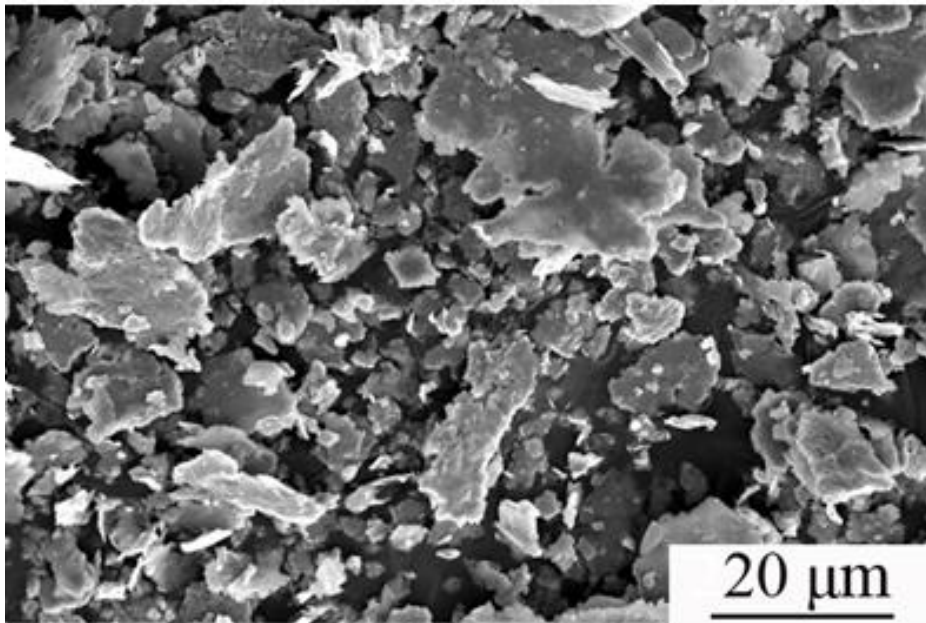


**Figure 3.4:** SEM micrograph of CrFeCoNiCu high entropy alloy powder milled at 65 h.

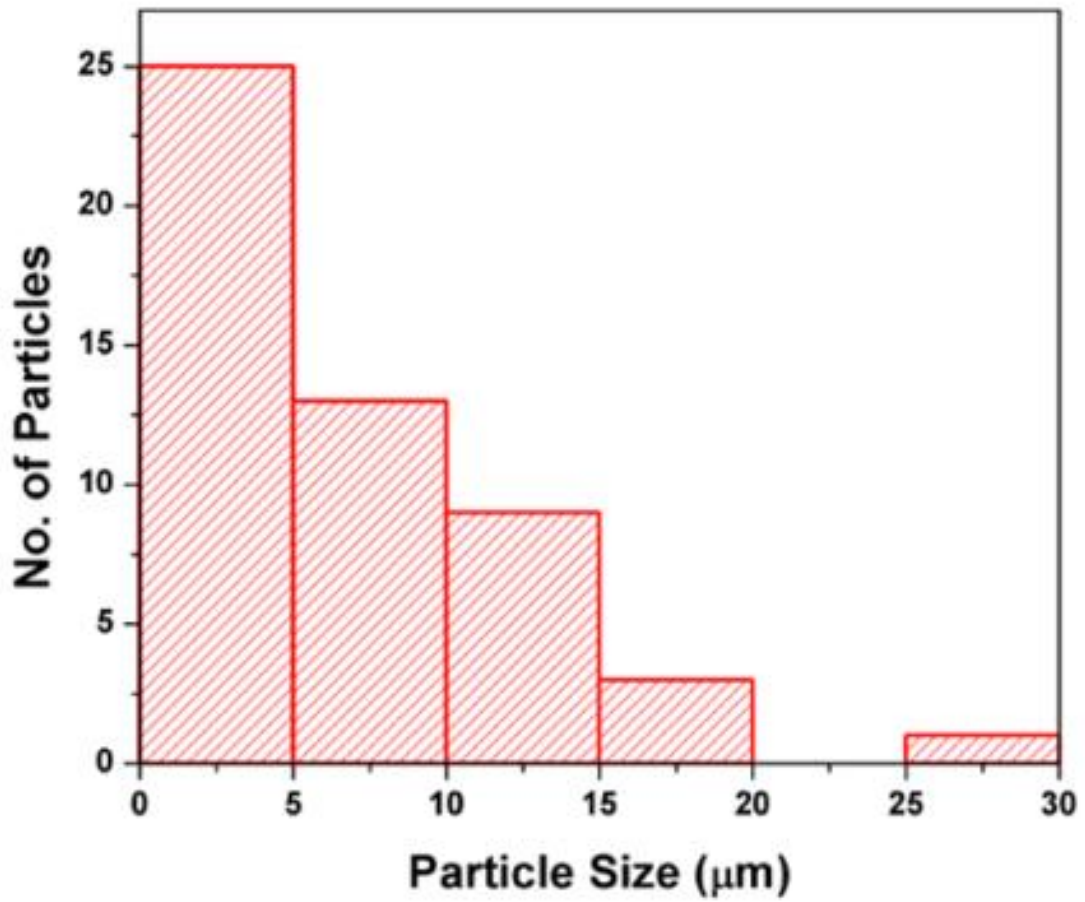


Figure 3.5: Particle size distribution observed in the SEM micrograph.

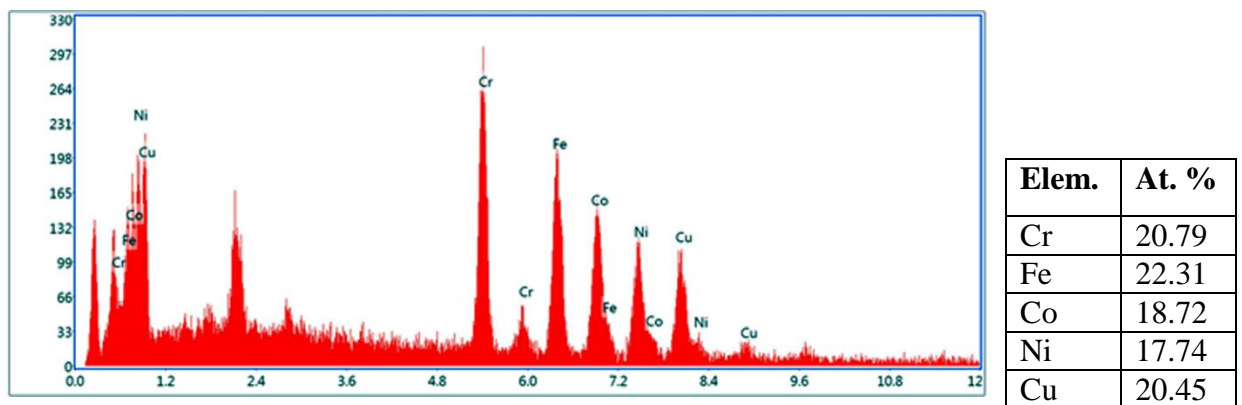
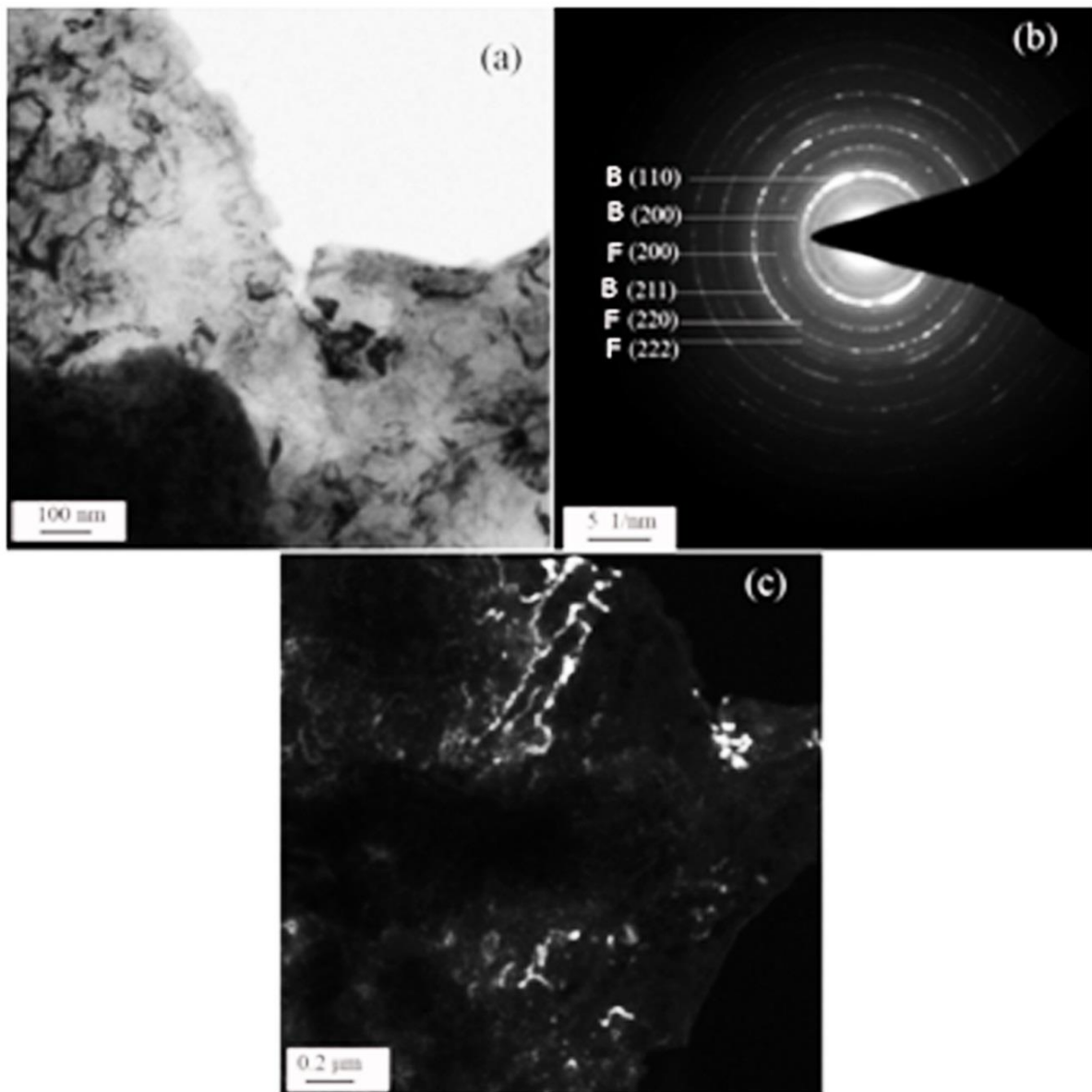
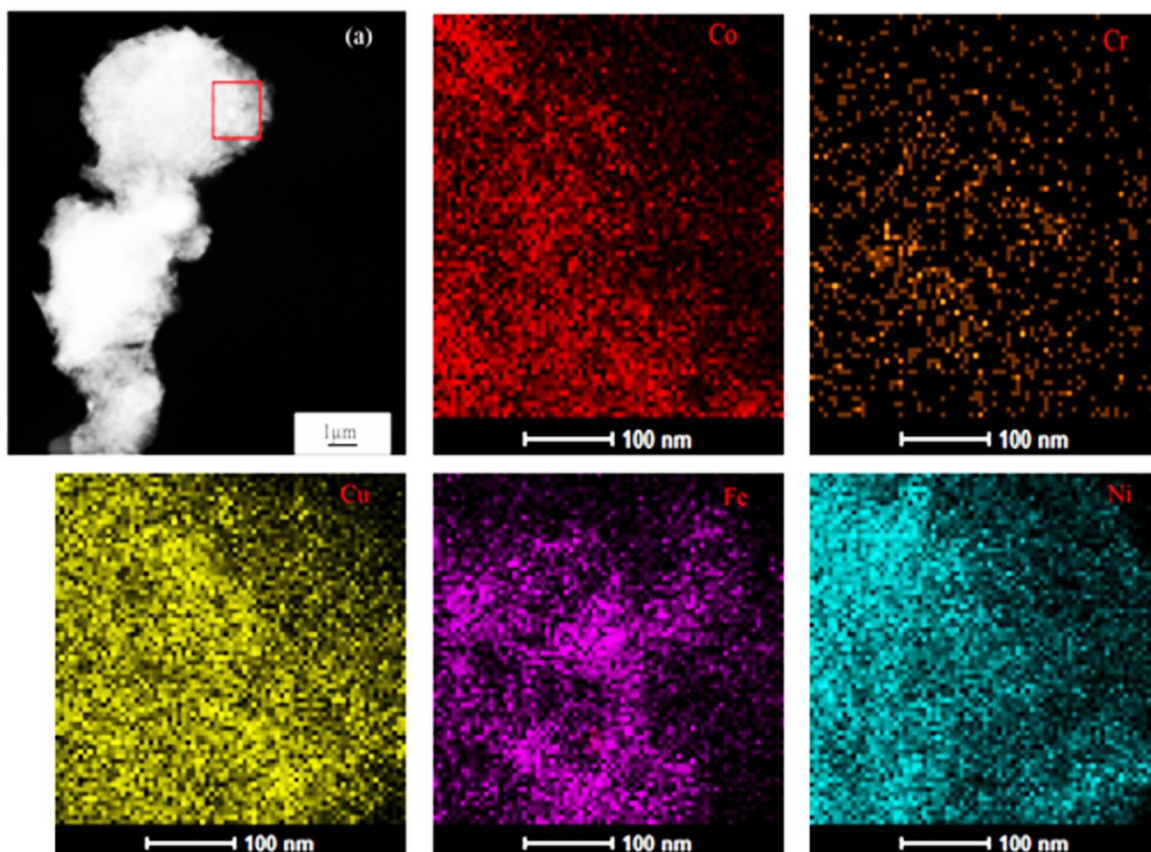


Figure 3.6: Elemental analysis of milled powder through EDX analysis.



**Figure 3.7:** TEM analysis of CrCoFeNiCu alloy. (a) Bright-field image (b) Indexed selected area diffraction (c) Dark-field image. Here, F and B indicates FCC and BCC respectively on the reflections in (b).



**Figure 3.8:** STEM-EDS elemental mapping of CrFeCoNiCu alloy showing Fe rich region.

### 3.4 Thermal stability of CrFeCoNiCu HEA

Diffusional transformations of phases in this HEA, is studied over a wide range of temperatures. The alloy was heated from room temperature to 900 °C (1173 K) in in-situ heating XRD. The X-ray diffraction patterns corresponding to various temperatures are shown in **Figure 3.9**. At room temperature, similar diffraction peaks are observed as that of the milled powder after 65 h of milling. We can observe that the sample is stable below 400 °C (673 K). Above this, new peaks become visible in the diffraction pattern ( $a = 8.45 \pm 0.02 \text{ \AA}$ ,  $c = 4.54 \pm 0.02 \text{ \AA}$ ) which closely matches with that of the ordered  $\sigma$  phase of Cr-Co/Fe. As the sample is further heated through 600 °C (873 K) to 900 °C (1173 K),

similar peaks with an increase in their integrated intensities are observed in the diffraction pattern. The intensity of peaks corresponding to the minor FCC phase was found to be increasing with temperature, indicating that more FCC phase is forming. This implies that the stable FCC phase is continuously evolving. This could be because the holding time in in-situ heating XRD is not enough to complete the formation of the FCC phase due to slow diffusion.

The powder sample was annealed at 1073 K for 2 h, analyzed by XRD (Figure 9) in order to confirm the equilibrium phases present. Two FCC phase ( $a = 3.62 \pm 0.02 \text{ \AA}$ ) and FCC2 ( $a = 3.61 \pm 0.02 \text{ \AA}$ ) got evolved along with a small amount of  $\sigma$  phase, while the BCC phase completely disappeared. It may be speculated that the  $\sigma$  phase may also disappear completely with sufficiently prolonged annealing. The CrFeCoNiCu alloys prepared by arc melting [32,105] and Laser cladding [106,107] have been shown to have FCC as a single stable phase. This indicates that the two FCC phases obtained after annealing of the 65 h milled powder at 1073 K for 2 h can be considered as a stable phases in this alloy.

For the precipitation temperature of the  $\sigma$  phase, milled powder was annealed at 623 K. XRD analysis of the annealed powder has shown a small amount of sigma phase formation at 623K, as can be seen from **Figure 3.10**. Thus, the onset temperature of the  $\sigma$  phase is approximately 623 K. The  $\sigma$  phase prone multi-component system can be predicted through VEC values ( $6.88 < \text{VEC} < 7.84$ ) [113]. In the present context, VEC value is indicating for  $\sigma$ -free phase, but we are obtaining the  $\sigma$  phase on annealing above 400 °C (673 K). It is shown that the VEC range for the  $\sigma$  phase formation with that for the mixed FCC and BCC solid solutions formation:  $6.87 \leq \text{VEC} \leq 8$ . [108]. Hence VEC parameters are not adequate for prediction of  $\sigma$  phase formation in the present alloy.

However, the formation of a two-phase mixture perhaps facilitates the formation of the  $\sigma$  phase.

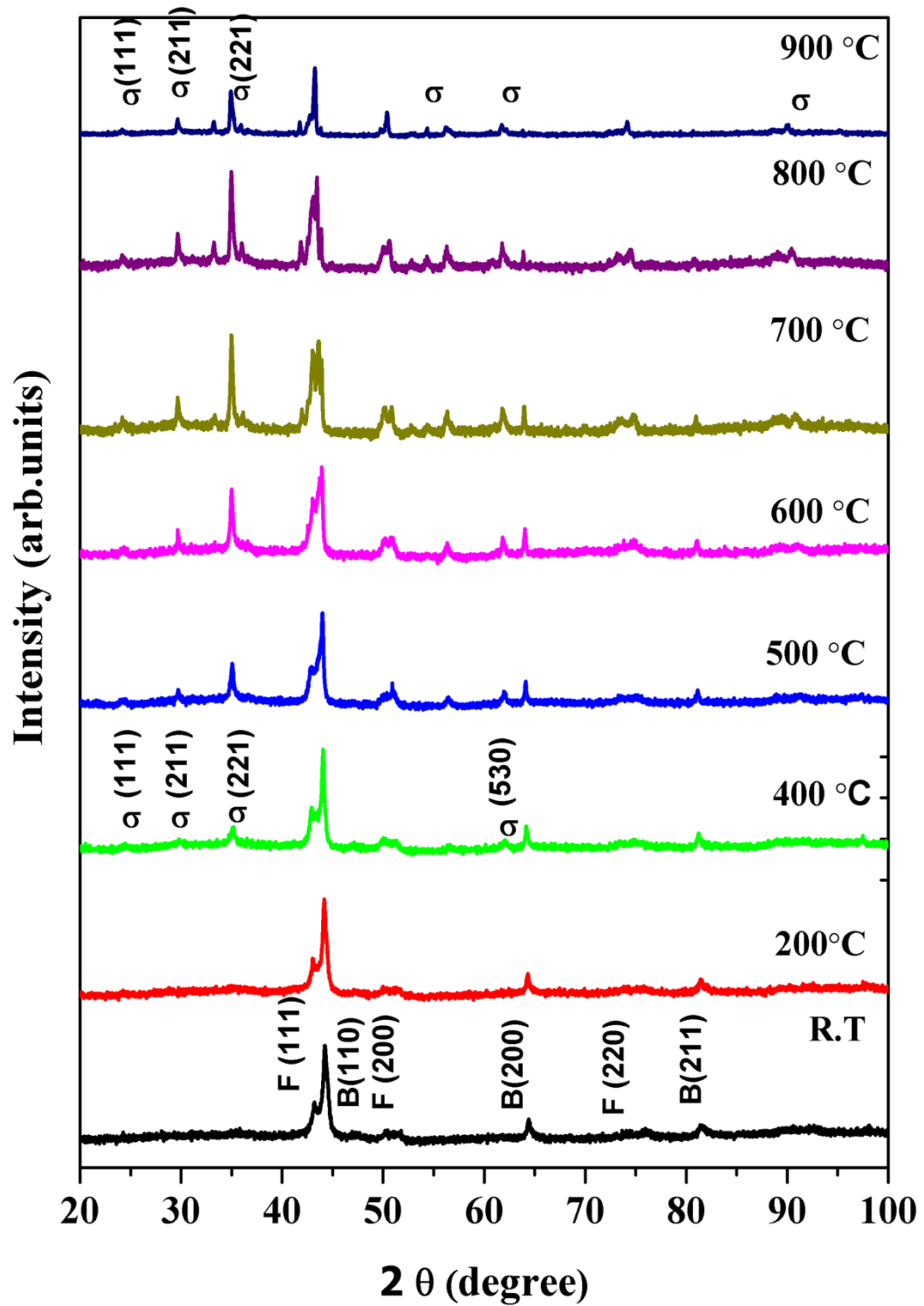


Figure 3.9: In situ high temperature XRD on as-milled powder.

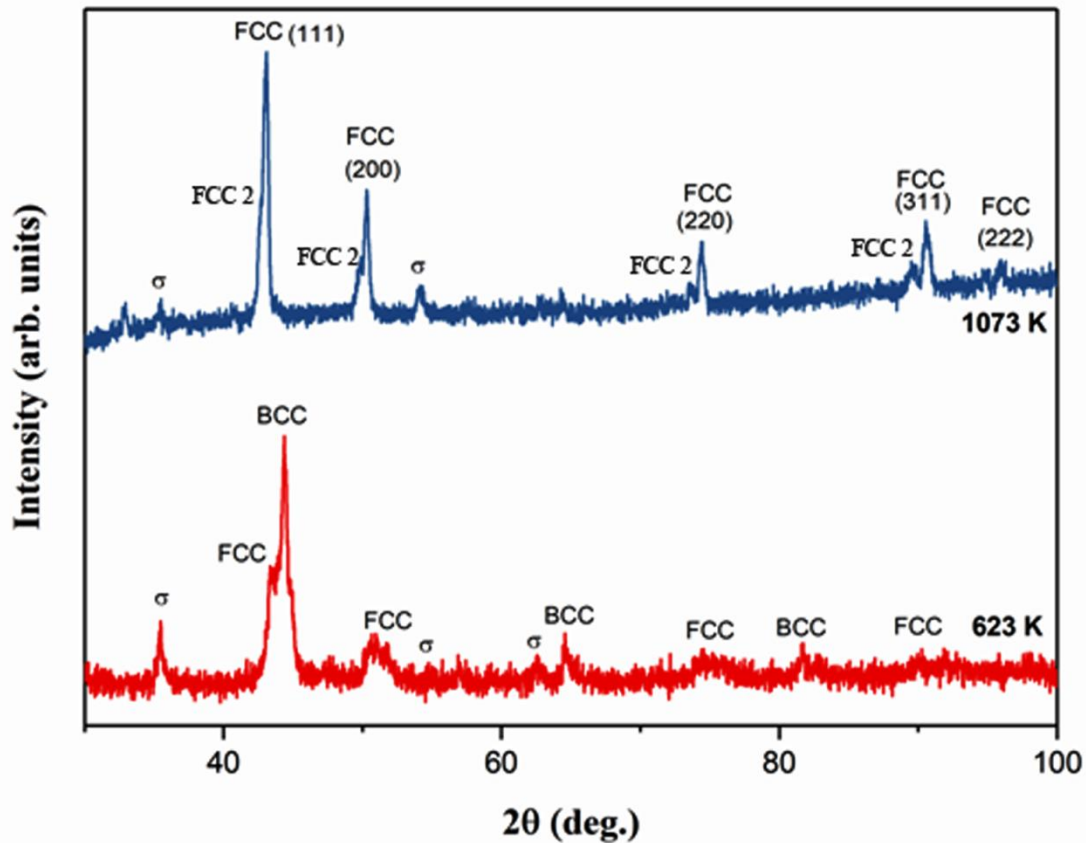


Figure 3.10: XRD patterns of annealed CrFeCoNiCu HEA powders at 623 and 1073 K.

### 3.5. Discussion

For the prediction of phases and their stability, we have performed some parametric calculations using formulae given in Section 3.1. The enthalpies of mixing for the binary system are calculated using Equation 3.1 and are tabulated in Table 3.2. The binary enthalpy values guide us in predicting the behavior of one element with the other constituent element in a multi-component alloy. From Table 3.3, we can expect Co-Fe, Co-Ni, Cu-Cr, Cu-Fe, Cr-Ni, and Fe-Ni has good mutual solubility, whereas Cu having significant positive enthalpy have a tendency of phase separation. According to Zhang et al. [47], the calculated parameters shown in Table 3.3 must lie within a specified range for solid solution formation, i.e., (i)  $\Delta S_{conf} \geq 13.38 \text{ Jmol}^{-1}\text{K}^{-1}$ , (ii)  $-10 \leq \Delta H_{mix} \leq 5 \text{ kJmol}^{-1}$



$^1\text{K}^{-1}$ , (iii)  $\delta \leq 6.6\%$ . Guo and Liu [36] have suggested additional criterion  $\text{VEC} > 8$ ,  $6.87 < \text{VEC} < 8$  and  $\text{VEC} < 6.87$  leads to the formation of FCC structure, a mixture of FCC and BCC structure, and BCC structure alone, respectively. The enthalpy of mixing, atomic size mismatch, and VEC values indicate FCC solid solution phase formation.

If we analyze the equilibrium phase diagram of CrFeCoNiCu (**Figure 3.1**), we can see the multiple phases at low temperatures. The reaction and the transformation temperature of phases from the equilibrium diagram (calculated using the CALPHAD approach) is summarized below

<b>Reactions</b>	<b>Temperatures (K)</b>
Liquid#2 $\rightarrow$ FCC_L12	1590
FCC_L12 $\rightarrow$ Liquid (Cu-rich)	1550
Liquid $\rightarrow$ FCC_ORD (Cu-rich)	1500
FCC_L12 $\rightarrow$ BCC_B2 (Cr-rich)	900
FCC_L12 $\rightarrow$ BCC_B2#2	790
FCC_L12 $\rightarrow$ FCC_L12#2 + FCC_ORD + BCC_B2 + BCC_B2#2	710

From the above description and **Figure 3.1** it is clear that the multiphase structure is stable at room temperature. The figure shows that FCC\_L12 dissolves completely into another FCC\_L12#2 structure along with a Cu-rich FCC\_ORD structure and two B2 phases. The composition of all the phases formed in the equilibrium diagram is tabulated in **Table 3.5**. From table one can easily understand that the FCC\_L12 structure at high temperature was composed of all elements except Cu, whereas FCC\_L12#2 structures formed at lower temperature has released Cr from its matrix. The rejected Cr leads

transform from disordered to ordered BCC\_B2 phase. The BCC\_B2#2 phase constitutes of Co and Fe as tabulated in **Table 3.5**.

The phases obtained in the milled powder after annealing it for two hours can be understood with the DFT and CALPHAD. As predicted by the DFT calculation, FCC is the stable structure. However, the enthalpy of mixing is positive, which indicates multiphase structures arising from phase separation at a lower temperature. The multiphase matrix is represented by the equilibrium diagram calculated using CALPHAD. The equilibrium diagram shows FCC\_L12 and Cu-rich FCC\_ORD phase as the major phase and two minor ordered BCC phases. The ordered FCC phase diffraction peaks are not present. This may be due to the sluggish diffusion of the elements in the multi-component alloy. Similar reason can be expected for missing peaks of B2 phase in the XRD analysis of annealed powder.

### 3.6. Conclusions

The following conclusions can be drawn from the present work

1. The semi-empirical parameters calculated for the prediction of phases such as enthalpy of mixing ( $3.2 \text{ kJ.mol}^{-1}$ ) and the weighted average of the atomic size difference (1.03) is within the solid solution-forming range ( $-10 \text{ kJ.mol}^{-1} < \Delta H_{mix} < 5 \text{ kJ.mol}^{-1}$ ) and mismatch factor  $\delta \leq 6.6$ ).
2. Enthalpy of mixing of the alloy for FCC phase calculated using DFT extrapolation of the enthalpy value of the FCC disordered 8 atom SQS of binary subsystems was found to be  $11.175 \text{ kJ.mol}^{-1}$ , which is lower than BCC and HCP structure at room temperature. The positive enthalpy value of FCC phase leads to the formation of multiple structures.

3. As per the prediction of CALPHAD approach, two ordered FCC and two ordered BCC phases were found to be stable below 450 °C, whereas two ordered FCC phases were stable above ~ 900 °C.
4. The nanostructured CrFeCoNiCu equiatomic alloy prepared by MA exhibited two phases, one with BCC crystal structure having lattice parameter  $a = 2.87 \pm 0.02 \text{ \AA}$  and a small amount of FCC phase having lattice parameter,  $a = 3.62 \pm 0.02 \text{ \AA}$ .
5. The BCC and FCC phases formed by MA were Fe-rich and Cu-rich, respectively as analyzed from STEM-EDS elemental mapping.
6. The synthesized HEA was revealed to be stable up to ~623 K and then due to transformations of  $\sigma$  phase precipitates by diffusion.
7. A simple FCC phase ( $a = 3.62 \pm 0.02 \text{ \AA}$ ) was obtained along with the FCC2 phase ( $a = 3.61 \pm 0.02 \text{ \AA}$ ) after annealing of the 65 h milled powder at 1073 K for two hours.
8. The VEC ranges for predicting  $\sigma$  phase formation are not observed to be applicable in the present alloy. However, the formation of a two-phase mixture is anticipated to facilitate the formation of the  $\sigma$  phase.

